Eigenmodes in a photonic structure with a torsion-deformed nematic liquid crystal exposed to a magnetic field

Vladimir A. Gunyakov ,[1,*] Alexander M. Parshin,[1,2] Ivan V. Timofeev ,[1,2] and Victor Ya. Zyryanov[1]
[1]*Kirensky Institute of Physics, Federal Research Center - Krasnoyarsk Scientific Center, Siberian Branch, Russian Academy of Sciences, Krasnoyarsk 660036, Russia*
[2]*Siberian Federal University, Krasnoyarsk 660041, Russia*

(Received 16 July 2020; accepted 9 September 2020; published 6 October 2020)

The polarized components of transmission spectrum of a multilayered photonic structure containing a nematic liquid crystal under the magnetic-field-induced torsion deformation have been investigated. Since the planarly twisted director structure of the nematic is unrelated to a decrease in its optical anisotropy, the control of the polarization and spectral characteristics of the eigenmodes is based on the occurrence of a geometric phase, whose contribution gradually increases upon nematic deformation. Along with the previously observed blue shift of the cavity *o* modes, the anomalous shift of the cavity *e* modes to the long-wavelength region (red shift) of the transmission spectrum has been detected. It has been shown that the countershift of the modes narrows the intermode interval. Remarkably, the extremal approaching of *e* and *o* modes in magnetic field H_{ex} occurs below the avoided crossing phenomenon observed in the stronger equalization field H_{eq} ($H_{ex} < H_{eq}$). The experimental results have been interpreted by the numerical simulation of the transmission spectra of the chiral photonic structure using the transfer matrix method.

DOI: 10.1103/PhysRevE.102.042701

I. INTRODUCTION

Multilayered photonic structures (PSs) of a Fabry-Pérot cavity type based on distributed Bragg mirrors evoke great interest as novel optical materials for creating functional elements of nanophotonics and optoelectronics devices [1,2]. These materials are characterized by the existence of photonic band gaps in the transmission spectrum. A defect that violates the PS periodicity leads to the appearance of narrow transmission peaks in the band gap, which are called defect (localized) modes. The use of anisotropic chiral media, for example, cholesterics [3] or twisted nematic liquid crystals (LCs), as defects gives rise to many intriguing polarization [4–6] and spectral [7–9] features in the optical response of the multilayered PSs.

As was shown using the coupled mode theory, in a twisted nematic Fabry-Pérot cavity, two normal propagation modes designated as twisted extraordinary (*te* mode) and twisted ordinary (*to* mode) [10] couple to each other upon reflection from mirrors and induce a cavity eigenmode [5]. In turn, the type (*re* or *ro*) of a resonant mode (cavity mode) and the state of its polarization relative to the local director **n** (the nematic optical axis) depend on the ratio between the amplitudes of the twisted modes that form the cavity mode. Despite the variable ellipticity of the *re* and *ro* modes in the medium, their polarization on mirrors is linear. This was theoretically established in Refs. [11–13] and experimentally confirmed in Ref. [14]. In the vicinity of the spectral points corresponding to the avoided crossing phenomenon, the directions of the linear polarization of the *re* and *ro* modes of neighboring series, being orthogonal, do not coincide with the directions parallel or perpendicular to the director on cavity mirrors. The maximum divergence between the polarization angles (±45°) and the director **n** is observed during the field-effect transition through these spectral points. In this case, the modes, when being as close as possible, exchange their states of polarization [8].

Another interesting phenomenon observed in the transmission spectra of the PSs with an anisotropic chiral medium is the anomalous shift of the *ro* mode to the short-wavelength region. Such shifts were observed by us, in particular, in the PSs with a nematic liquid crystal (PSLC) during the orientational transition from a hybrid to uniform twisted nematic configuration of the director [7], as well as upon excitation of the abnormal roll-type electroconvective instability in a planar aligned nematic layer [9]. It was established numerically and analytically that the blue shifts of the *ro* modes observed in these experiments are caused by the contribution of the geometric phase (GP) to the total phase change acquired by a mode for a round-trip propagation [7]. Unfortunately, the polarization optical properties of the nematic director configurations used in both cases limit the experiment capabilities and prevent studying the spectral behavior of the *re* modes, for which the anomalous shift to the long-wavelength spectral region was theoretically predicted [7].

A study of the above-mentioned polarization and spectral phenomena can be more informative for a PS with a planar aligned nematic layer under a magnetic field applied in the plane of this layer. If the magnetic field is perpendicular to the director **n** of a homogeneous LC layer, the orientational Fréedericksz transition occurs, which results in the torsion

*gun@iph.krasn.ru

 ©2020 American Physical Society

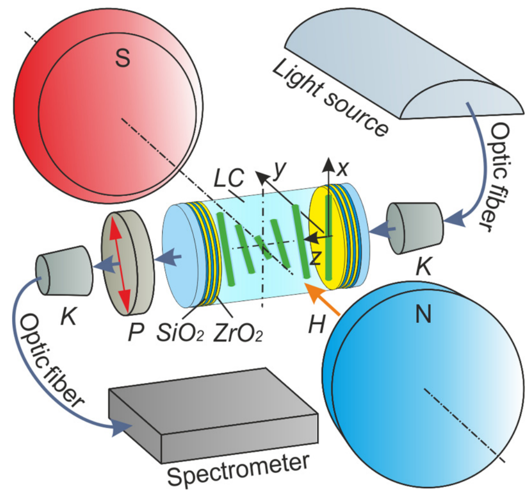

FIG. 1. Magnetooptical setup for studying the polarization and spectral characteristics of a multilayered photonic structure with a nematic LC in the torsion effect regime. Nematic molecules (shown by dashes) are initially aligned in the x-axis direction of the laboratory coordinate system, magnetic field H is directed along the y-axis, K are the collimators, and P is the polarizer.

deformation (the torsion effect [15]). A feature of the transition is that the structural transformations in a nematic LC are not accompanied by a decrease in the optical anisotropy of a medium. Therefore, any shifts of defect modes in the spectrum related to the change in the extraordinary refractive index are excluded. Hence, along with the blue shift of the *ro* modes, one can observe the countershift (red shift) of the *re* modes due to the GP contribution. In addition, it is important to understand how the coupling of the *o* and *e* modes propagating in a twisted medium affects the polarization state and spectral position of the cavity modes. The effect of mode coupling in the nematic layer under the magnetic-field-induced torsion deformation leading to the ellipticity of the linearly polarized incident light was described by Gerber and Schadt in Ref. [16]. This model is a generalization of the Mauguin's waveguide regime of the linearly polarized light propagation [17].

An input beam of light with its electric field vector $\mathbf{E} = (E_x, E_y)$ polarized along the x axis ($E_y = 0$) of the local coordinate system (x, y) falls on the planarly twisted nematic layer (Fig. 1); in the rotated system director $\mathbf{n}$ points always in the x direction. According to Ref. [16], the transverse electric field $E_y \neq 0$ can be shifted by a quarter period relative to the constant E_x component after exiting the layer, in general, the initial linear polarization is transformed to the elliptical one. The ellipticity of the output light depends on the parameter $w = k_0 d \Delta n / 2\pi$ here $k_0 = 2\pi/\lambda$ is the vacuum wave number, $\Delta n = n_e - n_o$ and d are the anisotropy of the nematic and its thickness, respectively. The ellipticity takes the maximum value at wavelengths $\lambda_{\max}$ at which the E_y function is maximal, near the values $w = 1, 2, 3, \ldots$ Further, the wavelengths $\lambda_{\max}$ are referred to as spectral points corresponding to Gerber-Schadt maxima condition. At the same time, there are the spectral points $\lambda_{\min}$ of the zero field E_y, which occur at the half-integer values of the parameter $w = 0.5, 1.5, 2.5, \ldots$. In spite of the elliptical polarization of light propagating through the twisted nematic the output polarization is linear at the wavelengths $\lambda_{\min}$. Since for the appropriate intensity the value $|E_y|^2 = 0$ is minimal, further these wavelengths are referred to as spectral points corresponding to Gerber-Schadt minima condition. It should be noted that the change of eigenmode (for the input light polarized along the y axis, i.e., perpendicularly to the director $\mathbf{n}$) leads to the same result of determining the Gerber-Schadt extrema. Thus, it should be expected that the polarization and spectral characteristics of the photonic structure with a torsion-deformed nematic are extremal at the wavelengths $\lambda_{\max}$ and $\lambda_{\min}$. Particularly, the intersection of the cavity modes at spectral points corresponding to the Gerber-Schadt minimum is an ordinary one. On the contrary, if the *re* and *ro* modes tend to intersect in the vicinity of a point corresponding to the maximum possible coupling of the *o* and *e* modes (Gerber-Schadt maximum), then we should expect the manifestation of the avoided crossing phenomenon, as in the case of a twisted nematic Fabry-Pérot cavity [8] during the field-effect transition through the Gooch-Tarry maximum [18].

In view of the aforesaid, here we examine the features of the polarization components of the transmission spectrum of a multilayered PS with a thin layer of a nematic twisted by a magnetic field in the spectral range between two Gerber-Schadt extrema. Then, the polarization and spectral behavior of the selected modes of orthogonal eigenpolarizations in the vicinity of the Gerber-Schadt maximum are examined. In this case, the spectral position of the modes is controlled by the contribution of the GP smoothly incoming since the moment of nematic twisting in a magnetic field above the Fréedericksz threshold. The spectra and state of polarization of the eigenmodes in the PSLC structure are detected by the rotating polarizer method upon their independent excitation. The experimental data are compared with the results of the numerical simulation by the 4 × 4 transfer matrix method.

II. EXPERIMENTAL

The spectral positions and polarization of the transmission peaks corresponding to eigenmodes of a PSLC structure under the torsion effect condition were experimentally investigated on a setup schematically shown in Fig. 1. The investigated multilayered PS is a microcavity consisting of two identical Bragg mirrors with a nematic liquid crystal layer as a structural defect between them: $(ZrO_2/SiO_2)^5ZrO_2$-LC-$ZrO_2(SiO_2/ZrO_2)^5$. The mirrors were formed by alternating vacuum deposition of zirconium dioxide (ZrO_2) with a refractive index of 2.04 and silicon dioxide (SiO_2) with a refractive index of 1.45 onto fused quartz substrates. According to the TEM data, the thicknesses of each of the six ZrO_2 layers and each of the five SiO_2 layers were (63 ± 5) nm and (82 ± 5) nm, respectively. The parameters of the PS were specified to form a first-order photonic band gap in the visible spectral range (424–624) nm with a set of resonance peaks corresponding to the modes localized on the nematic defect layer. The gap with a thickness of $d = (7.4 \pm 0.2)$ μm was filled with a 4-pentyl-4′-cyanobiphenyl (5CB) nematic liquid crystal. Polyvinyl alcohol (PVA) thin films were predeposited onto the mirror surfaces by a spin coating technique followed by unidirectional rubbing. The

PVA film ensures the uniform alignment of nematic molecules along the rubbing direction and their fairly strong anchoring to the mirror surface. The thermostatted PSLC cell was placed between the poles of an electromagnet, so that the nematic director **n** on the mirror surfaces was oriented along the x axis of the laboratory coordinate system (x, y, z). The electromagnet used could generate magnetic fields of up to $\sim$15 kOe directed parallel to the mirror planes along the y axis, i.e., perpendicular to the director **n** of the initially uniform nematic media. The value of magnetic field H was determined using a Hall effect sensor placed near the PSLC cell. The Hall voltage was detected with a 6-1/2 Digit Multimeter 34465A (Keysight Technologies). To obtain the H values in units of kOe, the Hall effect sensor was calibrated using a 421 Gaussmeter (Lake Shore Cryotronics Ins., Ohio, US). Above a certain threshold H_c value, the magnetic field can induce nonhomogeneous twisting of the nematic director **n** in the bulk of the LC layer by an angle of $\varphi = 90^\circ$ relative to the initial direction $\mathbf{n} \parallel x$ (the torsion effect).

The PSLC transmission spectra were recorded on a HR4000 spectrometer (Ocean Optics) under unpolarized illumination at a constant sample temperature $(26.0 \pm 0.2)^\circ$C. Polarizer P placed after the sample was used to detect both the polarization components $T_{||,\perp}(\lambda)$ of the PSLC transmission spectrum in zero field and the $T_{e,o}(\lambda)$ spectra corresponding to the states of polarization (SOPs) of eigenmodes in different fields $H > H_c$. Subscripts $||$ and $\perp$ denote the P orientation parallel and perpendicular to the initial orientation of the director **n**, respectively. Subscripts e and o denote the P orientation corresponding to maximum transmission on the wavelength of the selected *re* or *ro* modes, respectively. In the latter case, the angles between the linear polarization of the modes and the director **n** on the output mirror were determined simultaneously with the detection of the spectra. Note that, at the specified experimental parameters, the wave propagation in the PSLC structure does not correspond to the waveguide regime, since the cavity modes in the bulk of the field-twisted LC remain elliptically polarized [5,8]. As a polarizer, the Glan prism equipped with a limb and capable of rotating in the (x, y) plane was used. The radiation of a broadband light source was introduced into the sample and extracted from it to the spectrometer using optical fibers equipped with collimators.

III. RESULTS AND DISCUSSION

Figure 2 shows the polarization components $T_{||,\perp}(\lambda)$ of the PSLC transmission spectrum in the vicinity of the photonic band gap center obtained without field and in a fixed field of $H = 10.1$ kOe. The superimposed curves visualize the transformation of the polarization spectra upon twisting the nematic director by a magnetic field. The spectra of the PS with the nematic unperturbed by a field consist of well-resolved single peaks corresponding to the *re* modes [Fig. 2(a)] in the $T_{||}$ component and to the *ro* modes in the $T_\perp$ component [Fig. 2(b)]. Each set of the modes senses its refractive index, which is reflected in the difference between the intermode intervals: the presented spectral range contains eight peaks of the $T_{||}$ component and seven peaks of the $T_\perp$ component. It can be seen in Fig. 2 that the responses of the

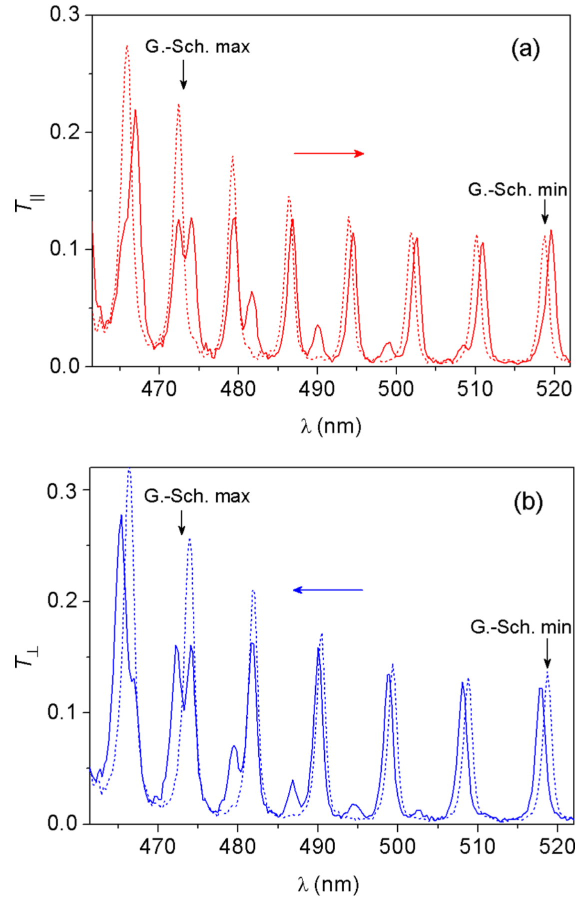

FIG. 2. Spectra of polarization components (a) $T_{||}(\lambda)$ and (b) $T_\perp(\lambda)$ without field (dashed lines) and in a field of $H = 10.1$ kOe (solid lines). Vertical arrows show the spectral points corresponding to the Gerber-Schadt extrema. Horizontal arrows show the cavity mode shift direction.

$T_{||}$ and $T_\perp$ polarization components to the field are essentially different. The $T_{||}$-component peaks in a field of $H = 10.1$ kOe were found to be shifted to the long-wavelength region [right-pointing arrow in Fig. 2(a)], while the $T_\perp$-component peaks, on the contrary, are shifted to the short-wavelength region [left-pointing arrow in Fig. 2(b)]. The near modes of both types are shifted by the same value relative to an initial position. A mechanism responsible for the observed anomalous shift of the PS modes under the torsion effect conditions is the incursion of the GP, which occurs during the nematic twisting by a field [7]. The multidirectional character of this shift is caused, in turn, by the GP contributions of different signs (plus for the *re* modes and minus for the *ro* modes) to the total phase change acquired by a mode for a round-trip propagation. At the same time, both components experience formally similar transformation of the transmission peak intensity between two specific spectral points $\lambda_{\max} = 473.2$ nm and $\lambda_{\min} = 518.8$ nm. An estimation of the parameter $w = k_0 d\Delta n/2\pi$ [16] using the dispersion dependences of the 5CB refractive indices [19] indicates that characteristics of the field-perturbed nematic structure in the investigated PSLC cell satisfy the Gerber-Schadt minimum condition ($w \sim 2.5$) at a wavelength of 518.8 nm and the Gerber-Schadt maximum condition ($w \sim 3.0$) at a wavelength of 473.2 nm. Figure 2 shows that at a fixed nematic twist angle specified by a field of 10.1 kOe the spectrum is mixed. Some satellite maxima arise near the eigenpeaks of each spectrum component between two Gerber-Schadt extrema. As the λ value decreases, smooth growth of the satellite maxima intensity is observed. The reason for the appearance of these maxima can be the smooth and unidirectional deviation of the linear polarization at the mirrors from the director **n** up to critical angles of $\pm 45^\circ$, at which the intensities of the eigenpeaks and satellites have to be equal (see, for instance, Ref. [14]). Indeed, the additional analysis of the mode polarization showed that the *re* and *ro* mode near a wavelength of $\lambda_{\min} = 518.8$ nm corresponding to single peaks are still polarized along and orthogonally to the **n** direction, respectively. At the same time, the *re* mode with 472.4 nm and the *ro* mode with 474.0 nm were found to be polarized at angles of $+45^\circ$ and -45° to the **n** direction, respectively; therefore, they manifest themselves similarly in the form of a doublet in each spectral component. Thus, for the latter pair of modes, a field of 10.1 kOe is the field H_{eq} of equalization of their intensities. In this case, the modes themselves are affected by the avoided crossing phenomenon, i.e., the repulsion of the orthogonally polarized eigenmodes approaching each other [14]. Instead of the expected crossing caused by the countershift, the modes resonate at the same frequencies as in zero field (Fig. 2). This is indicative of a balance of the mechanisms responsible for the approaching and repulsion of modes.

It should be noted that a decrease in the mode shift from ∼1 nm at the Gerber-Schadt minimum point to ∼0.4 nm at the Gerber-Schadt maximum point with increasing satellite peaks intensity (Fig. 2) is unrelated to the dispersion effects, since it occurs synchronously for the blue and red shifts. The observed deceleration of the shift probably originates from the polarization mode mixing, which increases upon approaching the Gerber-Schadt maximum point. As was mentioned above, the polarization of the eigenmodes of a doublet experiencing the avoided crossing made angles $\theta = \pm 45^\circ$ with the nematic director **n**. In particular, in the configuration presented in Fig. 1, the angle θ is determined experimentally from the angle of deviation of the transmission direction of the polarizing element from the initial direction $P \parallel x$ to the position corresponding to the maximum possible transmission $T \rightarrow T_{\max}$ at the frequency of this resonance. For the *re* modes, this is obtained by rotating the polarizer in the positive y-axis direction (the θ value with the plus sign is taken). For the *ro* modes, this is obtained by rotating P in the opposite direction (the θ value with the minus sign is taken). The corresponding $T_{e,o}(\lambda)$ spectra for the doublet modes selected in this way are presented in Fig. 3. In the polarizer position with $\theta = +45^\circ$, the eigenmode with $\lambda_e = 472.4$ nm corresponds to the single transmission peak T_e with the intensity much higher than that for the same wavelength in the doublet $T_{\parallel}$ [Fig. 3(a)]. The eigenmode with $\lambda_o = 474.0$ nm also corresponds to the high-intensity single peak T_o in the polarizer position with $\theta = -45^\circ$ [Fig. 3(b)]. It is noteworthy that the total quenching of the selected peaks is observed upon rotation of the polarizer by 90° from the desired polarization angle θ. The intermediate transmission peaks between the Gerber-Schadt extrema behave similarly: at a certain angle $\theta < 45^\circ$, each peak has the maximum intensity

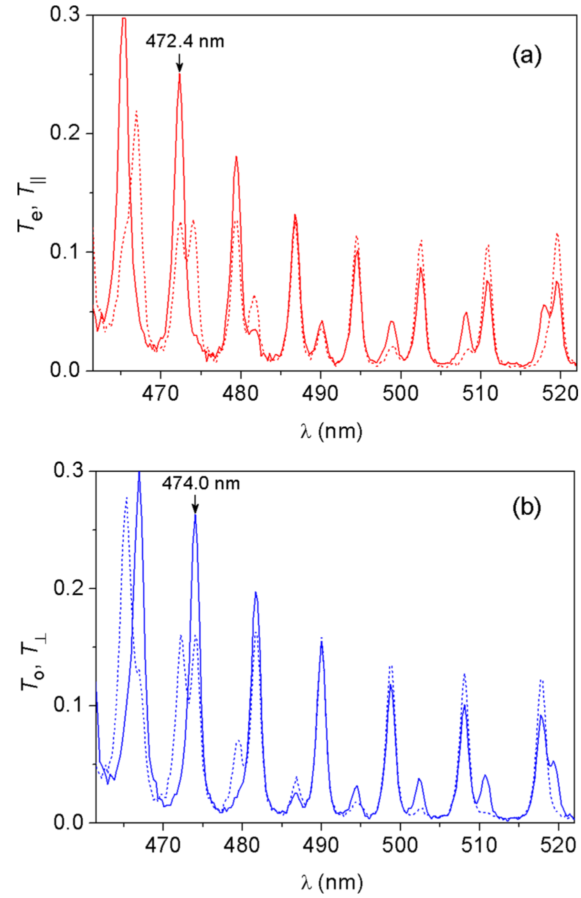

FIG. 3. $T_{e,o}(\lambda)$ spectra (solid lines) of the eigenmodes with (a) $\lambda_e = 472.4$ nm and (b) $\lambda_o = 474.0$ nm of the PSLC cell against the background of the corresponding polarization components $T_{\parallel,\perp}(\lambda)$ (dashed lines). All the spectra were obtained in a field of $H_{eq} = 10.1$ kOe.

and is completely extinguished at the orthogonal direction of the polarizer. This is indicative of the linear polarization of the eigenmodes on the PSLC cell mirrors under the torsion effect conditions. In the general case, the azimuth θ of the linear polarization of the resonance modes relative to the **n** direction on the mirrors can be arbitrary.

In view of the aforesaid, we consider in detail the mode doublet experiencing the avoided crossing in a field of $H_{eq} =$ 10.1 kOe, and the azimuthal variation of the linear polarization of each mode, i.e., the field-effect dynamics of the polarization upon twisting the nematic under the torsion effect conditions. To do that, the transmission peak of the eigenmode with $\lambda_e = 472.4$ nm or $\lambda_o = 474.0$ nm was tuned to the maximum possible value by the smooth rotation of the polarizer and the angle was read off by the limb of the polarization element. The procedure was performed over the entire accessible magnetic field range with a step of 0.47 kOe. The obtained field-effect dependences of the deviation angles $\theta(H)$ of the polarization of the doublet modes are presented in Fig. 4. The dependences reflect the threshold Fréedericksz transition ($H_c = 6.5$ kOe) for the torsion deformation of the nematic [15] and allow us to follow the evolution of the SOP modes with increasing field. In the fields below the Fréedericksz

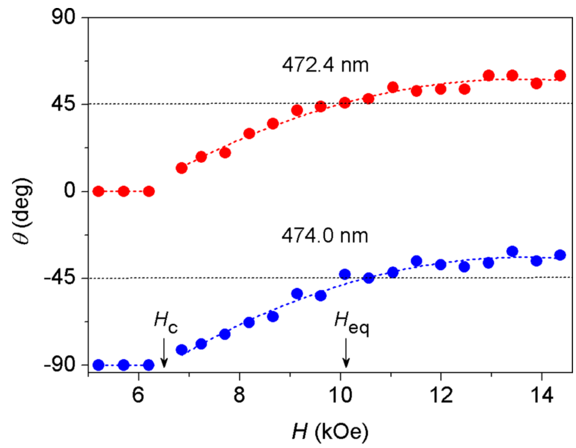

FIG. 4. Field-effect dependences of the angles of deviation of the linear polarization $\theta(H)$ from the director **n** on the PSLC cell output mirror for the modes with $\lambda_e = 472.4$ nm (red circles) and $\lambda_o = 474.0$ nm (blue circles) experiencing the avoided crossing ($\theta = \pm 45^\circ$) in a field of $H_{eq} = 10.1$ kOe. The threshold Fréedericksz transition field is $H_c = 6.5$ kOe. Dashed lines correspond to the interpolation.

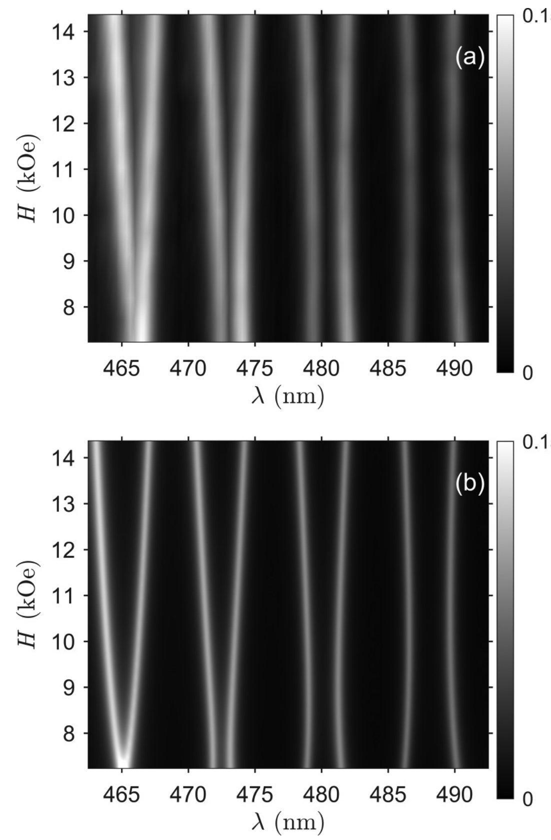

FIG. 5. Grayscale patterns of the (a) experimental and (b) calculated unpolarized transmission spectra of the PSLC cell given as functions of wavelength and applied magnetic field. The bars on the right indicate the transmittance value.

transition ($H < H_c$), the *re* and *ro* modes remain linearly polarized along the axes $x \parallel \mathbf{n}$ ($\theta = 0^\circ$) and y ($\theta = -90^\circ$), respectively. Above the threshold, with an increase in H, one can observe the unidirectional deviation of the linear polarization from the coordinate axes, up to critical angles of $+45^\circ$ for the *re* mode and -45° for the *ro* mode at $H = H_{eq}$, which leads to the polarization mode mixing. The crossing of critical levels of $\pm 45^\circ$ by the $\theta(H)$ dependences demonstrates the synchronous transformation of the SOPs: $re \rightarrow e2o \rightarrow ro$ for the λ_e mode and $ro \rightarrow o2e \rightarrow re$ for the λ_o mode. Above H_{eq}, with a further increase in the field, the SOPs change insignificantly and shift toward the corresponding axes: $\theta \rightarrow +90^\circ$ (y axis) for the *re* modes and $\theta \rightarrow 0^\circ$ (x axis) for the *ro* modes. These dependences evidence for the synchronous evolution of the SOPs of the eigenmodes with $\lambda_e = 472.4$ nm and $\lambda_o = 474.0$ nm over the entire accessible field range. In this case, the modes remain orthogonally polarized, regardless of the field value and, consequently, the nematic twist angle.

Figure 5 presents the experimental and calculated plots illustrating the transformation of the PSLC cell transmission spectrum in fields of $H = (6.5–14.2)$ kOe in the gray scale. The spectra were recorded with a step of 0.47 kOe at a constant temperature of $(26.0 \pm 0.2)^\circ$C [Fig. 5(a)]. The numerical simulation of the spectra with account taken of the light wave field attenuation in a layered structure and the dispersion of the LC material was performed using the approach described in detail in Ref. [13]. Using the procedure of minimizing the free energy of the director field $\mathbf{n}(\mathbf{r})$, the orientation structure of the nematic inside the defect layer in zero and nonzero magnetic field was calculated. Then, using the 4×4 transfer matrix method [20], the transmission of the polarized light through the investigated multilayered structure was simulated. Figure 5(b) shows the PSLC-cell transmission spectra obtained in this way. One can see good agreement between the experimental and calculated field-effect dependences of the spectral positions of the modes in the narrowed range inside the photonic band gap

It is noteworthy that up to a threshold field of $H_c = 6.5$ kOe, the *re* modes of all pairs of the chosen spectral range are localized on the left of the *ro* modes. Thus, the nematic twisting should lead to a decrease in the intermode interval for all pairs of the orthogonal polarized modes due to their approaching (Fig. 2). However, in the vicinity of the Gerber-Schadt maximum point in the spectrum, the pairs show different shift dynamics. Initially the closely approached modes with $\lambda_e = 465.7$ nm and $\lambda_o = 466.5$ nm of the short-wavelength pair undergo the SOP transformation $re \leftrightarrow ro$, experiencing the avoided crossing at an equalization field of $H_{eq} = 7.5$ kOe. Therefore, almost immediately, the modes diverge each according to its GP incursion. At the same time, the investigated doublet $\lambda_e = 472.4$ nm and $\lambda_o = 474.0$ nm resonates at constant wavelengths in fields of up to ∼8.0 kOe, which is caused by the balance of mechanisms responsible for approaching and repulsion of modes. In the range of (8.0–10.1) kOe, the repulsion caused by the increasing coupling of modes on the mirrors starts dominating [5]. Therefore, above an extreme proximity field of $H_{ex} = 8.0$ kOe, the modes diverge. However, in a field of H_{ex}, the polarization exchange typical of the avoided crossing does not occur between modes yet. For example, the mode with $\lambda_e = 472.4$ nm, which resonates on the left, retains SOP as *re* mode, in spite of the incursion of its

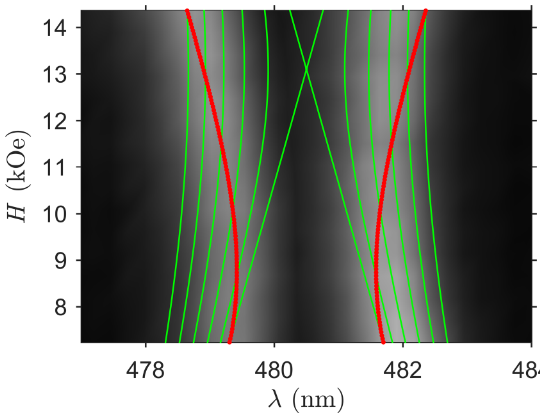

FIG. 6. Against the background of experimental transmittance (grayscale pattern), analytical trajectories (1) of spectral positions of the maxima of the eigenmodes with $\lambda_e = 479.3$ nm and $\lambda_o = 481.7$ nm for the increasing (red curves) and constant (series of green curves) mode coupling coefficient are plotted as functions of applied magnetic field.

own GP, starts shifting to the short-wavelength spectral region, i.e., demonstrates a paradoxical inverse shift. The mode with $\lambda_o = 474.0$ nm behaves similarly. When an equalization field of $H_{eq} = 10.1$ kOe is attained, the transformed doublet modes (see Fig. 4) continue diverging in the previous direction, but now each mode shifts according to the incursion of its GP. It can be seen in Fig. 5 that the third ($\lambda_e = 479.3$ nm and $\lambda_o = 481.7$ nm) and fourth ($\lambda_e = 486.7$ nm and $\lambda_o = 490.5$ nm) pairs of modes approach each other in weak fields. Then the mode trajectories clearly show the points of extrema approaching $H_{ex3} = 8.5$ kOe and $H_{ex4} = 11.0$ kOe, respectively, at which the mode repulsion effect prevails over the mechanism of their approaching. This, in turn, causes a paradoxical inverse shift of the modes until attaining the equalization fields. For example, for the third pair, the equalization field was $H_{eq} = 13.0$ kOe. The equalization field of the fourth pair apparently goes beyond the limits of magnetic fields that can be used in the experiment. Thus, the transformation of the SOP of the diverging modes at the equalization fields smoothly restores the correct field-effect dynamics of their spectral positions. Passing to Fig. 5, we should emphasize an important feature in the behavior of the PSLC eigenmodes under the torsion effect conditions. In contrast to the case of a twisted nematic Fabry-Pérot cavity [8], the mode intensity equalization field H_{eq} and, correspondingly, the avoided crossing point, seem, in all the cases, to be delayed from the field H_{ex} of the extremal approaching of the modes.

Figure 6 shows trajectories of spectral positions of the maxima of the eigenmodes with $\lambda_e = 479.3$ nm and $\lambda_o = 481.7$ nm (red curves) that reflect the experimental field-effect dynamics of the transmission spectrum (grayscale pattern as a background) over the entire accessible magnetic field range. The trajectories are analytically described by the conventional avoided crossing formula. See, for example, Eq. (26) in Ref. [7] that can be simplified as:

$$\lambda^{\pm} = \frac{\lambda_e + \lambda_o}{2} \pm \sqrt{\kappa^2 + \alpha(H - H_{eq})^2}, \quad \kappa(H) = \beta H, \quad (1)$$

where κ is the mode coupling coefficient that grows proportional to applied field H. When the coefficient κ is constant with the field, the dependence $\lambda(H)$ gives a hyperbola with the center at $H = H_{eq}$. A series of green trajectories in Fig. 6 corresponds to different κ values: a certain coupling coefficient corresponds to each pair of symmetric hyperbolas. The stronger is coupling, the larger is the distance between the modes $\lambda^+ - \lambda^-$. The crossover at a point of $H_{eq} = 13.0$ kOe corresponds to the crossing of partial eigenmodes without coupling at the mirrors. The variation of the coefficient κ with the field yields hyperbolas with the shifted center at $H_{ex} = 8.5$ kOe (red curves). In the real experiment, the extremal approaching of the PSLC structure modes under the torsion effect conditions is observed before the avoided crossing phenomenon ($H_{ex} < H_{eq}$), in contrast to the previous investigations ($H_{ex} = H_{eq}$) [8,14]. The observed delay is easy to explain. An increase in the field strength leads to an increase in the degree of nematic twisting and occurrence of the GP incursion, which induces approaching of the cavity modes of the orthogonal eigenpolarizations. Such approaching in the vicinity of spectral point corresponding to the Gerber-Schadt maximum leads to the strong polarization mixing of the elliptically polarized twisted *te* and *to* modes. At the same time, the strength of their coupling sharply increases at a growth rate of much higher than the rate of the transformation of the SOPs of the *re* and *ro* modes. This eventually results in the uncorrelated field-effect dynamics of the spectral positions of the cavity modes and their SOPs.

IV. CONCLUSIONS

The polarization and spectral characteristics of the eigenmodes of a multilayered photonic structure with a nematic under the conditions of the magnetic-field-induced torsion deformation were experimentally and theoretically investigated. In the region of the transmission spectrum between the two Gerber-Schadt extrema, the polarization mode mixing was detected. The anomalous countershifts of the defect modes of the orthogonal eigenpolarizations were demonstrated, which are caused by the contribution of the geometric phase incoming from the moment of twisting of the nematic above the threshold field of the Fréedericksz transition. The linear character of the polarization of the *re* and *ro* modes at the mirrors and the synchronous transformation of their polarization states during the field-effect transition through the Gerber-Schadt maximum critical point were established. Similar to the mode dynamics of a twisted nematic Fabry-Pérot cavity, at this critical point, the eigenmodes of the investigated photonic structure transform to their opposites, remaining orthogonally polarized. At the same time, a specific character of the field-induced torsion effect manifests itself in a different dependence of the polarization angles of the modes, which reflects the behavior of the critical parameters at the Fréedericksz transition [21]. In addition, a specific character manifests itself in the uncorrelated field-effect dynamics of the polarization states and spectral positions of the modes. In particular, it was found that the extremal approaching of the modes of orthogonal eigenpolarizations occurs much earlier than the avoided crossing phenomenon observed in the equalization field ($H_{ex} < H_{eq}$). This is caused by the dependence of the coupling between the modes on the applied field, i.e., the competition between the countershift and repulsion of the *re* and *ro* modes. The latter mechanism is determined by the strength of coupling between the elliptical twisted modes forming each cavity mode. The obtained experimental results were confirmed by the numerical simulation of the transmission spectra of the PSLC structure under the torsion effect conditions using the 4×4 transfer matrix method. It should be noted that the magnetic field was used for convenience of measurements. Analogous results can be obtained by applying an electric field instead of the magnetic field for the torsion deformation of the homogeneous nematic layer. Then the proposed alternative method for controlling the polarization and spectral characteristics of eigenmodes of the chiral photonic structures, which is unrelated to the decrease of the optical anisotropy, can be used in polarization splitting and rotation, filtering, switching, and optical modulation of light fluxes in photonics and optoelectronics devices.

ACKNOWLEDGMENT

I.V.T. acknowledges the support by RFBR 19-52-52006.

[1] J. D. Joannopoulos, R. D. Meade, and J. N. Winn, *Photonic Crystals: Molding the Flow of Light* (Princeton University Press, Princeton, 1995).
[2] K. Busch, G. von Freymann, S. Linden, S. F. Mingaleev, L. Tkeshelashvili, and M. Wegener, Phys. Rep. **444**, 101 (2007).
[3] V. A. Belyakov, *Diffraction Optics of Complex-Structured Periodic Media* (Springer International Publishing, Cham, 2019).
[4] J. S. Patel and Y. Silberberg, Opt. Lett. **16**, 1049 (1991).
[5] Y. Ohtera, H. Yoda, and S. Kawakami, Opt. Quantum Electron. **32**, 147 (2000).
[6] A. H. Gevorgyan, M. Z. Harutyunyan, K. B. Oganesyan, and M. S. Rafayelyan, Optik. **123**, 2076 (2012).
[7] I. V. Timofeev, V. A. Gunyakov, V. S. Sutormin, S. A. Myslivets, V. G. Arkhipkin, S. Y. Vetrov, W. Lee, and V. Y. Zyryanov, Phys. Rev. E **92**, 052504 (2015).
[8] V. A. Gunyakov, I. V. Timofeev, M. N. Krakhalev, W. Lee, and V. Y. Zyryanov, Sci. Rep. **8**, 16869 (2018).
[9] V. A. Gunyakov, M. N. Krakhalev, I. V. Timofeev, V. Y. Zyryanov, and V. F. Shabanov, Opt. Mater. **100**, 109630 (2020).
[10] P. Yeh and C. Gu, *Optics of Liquid Crystal Displays*, Wiley Series in Pure and Applied Optics (Wiley, New York, 1999).
[11] H. Yoda, Y. Ohtera, O. Hanaizumi, and S. Kawakami, Opt. Quantum Electron. **29**, 285 (1997).
[12] X. Zhu, Q. Hong, Y. Huang, and S.-T. Wu, J. Appl. Phys. **94**, 2868 (2003).
[13] I. V. Timofeev, Y.-T. Lin, V. A. Gunyakov, S. A. Myslivets, V. G. Arkhipkin, S. Y. Vetrov, W. Lee, and V. Y. Zyryanov, Phys. Rev. E **85**, 011705 (2012).
[14] V. A. Gunyakov, I. V. Timofeev, M. N. Krakhalev, and V. Y. Zyryanov, Phys. Rev. E **96**, 022711 (2017).
[15] L. M. Blinov, *Structure and Properties of Liquid Crystals, Topics in Applied Physics* (Springer, Berlin, 2010).
[16] P. R. Gerber and M. Schadt, Z. Naturforsch., A. **35**, 1036 (1980).
[17] C. V. Mauguin, Bull. Soc. Fr. Miner. **34**, 71 (1911).
[18] C. H. Gooch and H. A. Tarry, J. Phys. D: Appl. Phys. **8**, 1575 (1975).
[19] S.-T. Wu, C.-S. Wu, M. Warenghem, and M. Ismaili, Opt. Engineering. **32**, 1775 (1993).
[20] D. W. Berreman, J. Opt. Soc. Am. **62**, 502 (1972).
[21] E. Guyon, Am. J. Phys. **43**, 877 (1975).